Optics and Spectroscopy, 2024, Vol. 132, No. 8

01

Balanced detection of linear dichroism signals in cesium

© *A.K. Vershovskii, A.S. Pazgalev, M.V. Petrenko*

Ioffe Institute, St. Petersburg, Russia

e-mail: antver@mail.ioffe.ru

Received August 15, 2024
Revised August 15, 2024
Accepted August 26, 2024

We present the results of a theoretical and experimental comparison of methods for recording linear dichroism signals that arise in saturated alkali metal vapor (cesium) under the influence of linearly polarized light propagating perpendicular to the magnetic field. Such signals are of both fundamental and applied interest, primarily for the implementation of new laser frequency stabilization methods based on atomic transitions. In addition to the standard method of measuring the full intensity of the probe light, we investigated the balance detection method, widely used for detecting circular birefringence signals; its main advantage is that it suppresses laser intensity noise. It is shown that when recording linear dichroism signals, the use of this method can also provide an advantage in signal-to-noise ratio. The use of balanced schemes opens up additional possibilities for the application of the linear dichroism effect.

Keywords: linear dichroism, optical alignment, linearly polarized light, transverse magnetic field, balanced signal detection.

DOI: 10.61011/EOS.2024.08.60034.6982-24

Introduction

Studies of spin effects induced in atomic media (and their nearest analogs such as color centers in crystals, quantum dots, etc.) by resonance radiation are currently becoming increasingly important. Fundamental interest in this topic is associated with the avalanche growth of applications such as quantum sensorics [1], quantum interferometry [2,3], quantum informatics [4], laser cooling methods [5] and many more. The overwhelming majority of studies are devoted to the optical orientation effects — a process when atoms exposed to circularly polarized light acquire a non-zero collective magnetic moment, or to two-photon effects (coherent population trapping, EIT, etc.) [6–8].

However, optical orientation is not the only possible result of optical pumping, but is just the first in the similar effect hierarchy. As is commonly known, linearly polarized light induces in the atomic medium placed in a magnetic field a so-called alignment — a non-equilibrium state defined by symmetric distribution of populations over magnetic sublevels (as opposed to orientation with its maximum asymmetric atom distribution over sublevels). For more rigorous definition of alignment and its difference from higher-order distributions, see [9,10].

It follows from the above that alignment, as opposed to orientation, is not followed by a non-zero magnetic moment occurring in a medium; this renders some methods used to detect orientation unsuitable for alignment detection. Therefore the alignment effects have not been used so widely as the orientation effects. Nevertheless, the Voigt geometry, where a beam propagates along the z axis perpendicularly to a magnetic field (MF) with the vector of which the x axis direction is associated, provides effective detection of alignment signals by test radiation absorption.

Investigation of effects induced by linearly polarized light is of interest for various reasons with the following one being the most substantial among them: using linearly polarized pumping in the Voigt-geometry makes it possible to handle the relative position of the polarization plane and MF direction — which is impossible with circularly polarized light pumping. And this in turn makes it possible to control alignment in a system and record time-varying linear dichroism (LD) signals not related to magnetic resonance. Such signals, in particular, were experimentally studied in [11] and used for laser frequency stabilization without modulation.

The objective of this work is to perform theoretical analysis and experimental study of LD signals in alkali metal (Cs) vapor exposed to linearly polarized resonance light, and to compare various signal detection methods. An expected result of such study implies enhancement of LD effect application capabilities, primarily for laser frequency stabilization tasks. The study will investigate the applicability of balanced schemes (see, for example, [12,13]) for LD detection. Such balanced schemes that actually measure the rotation angle of the polarization plane of the probe light are widely used to detect circular birefringence signals under circularly polarized light pumping. They ensure effective laser noise suppression and, therefore, can also provide additional applicability of the LD effect.

Experimental study of alignment signals in this work has been conducted in the most interesting from a practical standpoint single-beam scheme where a pumping beam serves as a detecting (probe) beam at the same time.

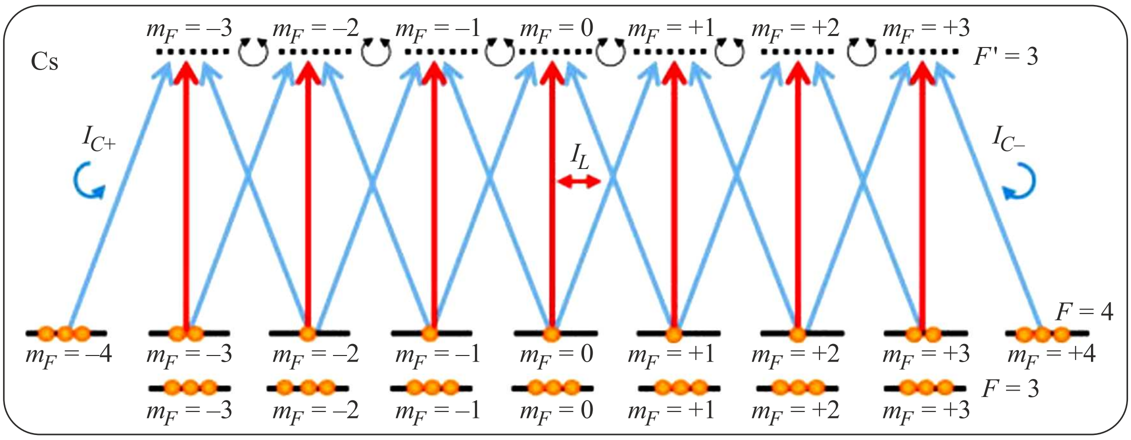

Figure 1. Scheme of levels and transitions in Cs during pumping and detection by the linearly polarized light on the line $F = 4 \leftrightarrow F' = 3$.

Theory

Let's consider a so-called double-beam scheme where a strong pumping beam and weak probe beam pass through an atomic medium. Let both these beams propagate along the z axis and weak MF is directed along the x axis. In such system, LD is displayed as a difference in the absorption coefficients K_x and K_y measured by a weak test beam whose linear polarization vector is directed consecutively along the system's x and y axes.

Transmission of weak test light with an arbitrary polarization azimuth φ_0 through the medium is described using the Jones calculus as follows:

$$\begin{pmatrix} E_x \\ E_y \end{pmatrix} = \mathbf{T} \cdot \begin{pmatrix} E_{0x} \\ E_{0y} \end{pmatrix}, \qquad (1)$$

where $E_{0x} = E_0 \cos(\varphi_0)$, $E_{0y} = E_0 \sin(\varphi_0)$, e_0 is the amplitude of the electric component of light wave, $\mathbf{T}$ is the Jones matrix containing the transmission coefficients T_{ij}. We'll assume below that the $\mathbf{T}$ matrix elements are real (i.e. there is no birefringence), off-diagonal elements are equal to zero — which follows from the symmetry of the studied system (second-order symmetry occurring when there is one preferred axis x):

$$\mathbf{T} = \begin{pmatrix} T_{xx} & 0 \\ 0 & T_{yy} \end{pmatrix} = \begin{pmatrix} \sqrt{1-K_x} & 0 \\ 0 & \sqrt{1-K_y} \end{pmatrix}. \qquad (2)$$

The absorption coefficients of light polarized along the x and y axes of the coordinate system are generally not equal and we may introduce a concept of an absorption vector $\mathbf{K}$ with components K_x and K_y. The polarization intensity and azimuth at the input and output of the medium are equal respectively, to

$$I_0 = E_{0x}^2 + E_{0y}^2 = I_{0x} + I_{0y}, \quad I = E_x^2 + E_y^2 = I_x + I_y$$

$$\varphi_0 = \arctan\left(\frac{E_{0y}}{E_{0x}}\right), \quad \varphi = \arctan\left(\frac{E_y}{E_x}\right). \qquad (3)$$

In general, the rotation of the plane of polarization of radiation is equal to $\Delta\varphi = \varphi - \varphi_0 \neq 0$. Intensities of the beam components characterized by polarization along the x and y axes of the coordinate system are, respectively, equal to

$$I_{0x} = I_0 \cdot \cos^2(\varphi_0), \quad I_x = I \cdot \cos^2(\varphi)$$

$$I_{0y} = I_0 \cdot \sin^2(\varphi_0), \quad I_y = I \cdot \sin^2(\varphi). \qquad (4)$$

In a multilevel system featuring linear dichroism, the absorption coefficient components K_x and K_y depend on pumping conditions in a complicated way. ΔK of the LD effect is defined by the relative difference of the absorption coefficients: $\Delta K = (K_x - K_y)/(K_x + K_y)$.

Let's consider a cell with alkali atoms and buffer gas; the buffer gas pressure will be assumed sufficient to ensure complete mixing of excited atom states in collisions with gas atoms (or molecules). This implies partial or full overlapping of absorption profiles of the lines $F = I + 1/2 \leftrightarrow F' = I - 1/2$ and $F = I + 1/2 \leftrightarrow F' = I + 1/2$. The scheme of Cs ($I = 7/2$) atom levels in the simplest case, i.e. in pumping and detecting by linearly polarized light on the line $F = 4 \leftrightarrow F' = 3$, is shown in Figure 1.

Here, the vertical arrows show the linearly polarized light (a pumping component polarized along the x axis), inclined arrows show the counterclockwise-polarized and clockwise-polarized light into which the pumping component polarized along the y axis is expanded. Transition probabilities are defined by the Clebsch–Gordan coefficients [14]. Double arc-shaped arrows denote mixing of excited states. The scheme includes 16 ground state levels. Excited state populations will be hereinafter assumed equal to zero. Pumping schemes on the other three transitions of the D_1 line of Cs look similarly.

Population distribution in such system (assuming that there are no any coherences in the ground state and the excited state levels are fully mixed) may be calculated by solving a system of balanced equations. For the ground

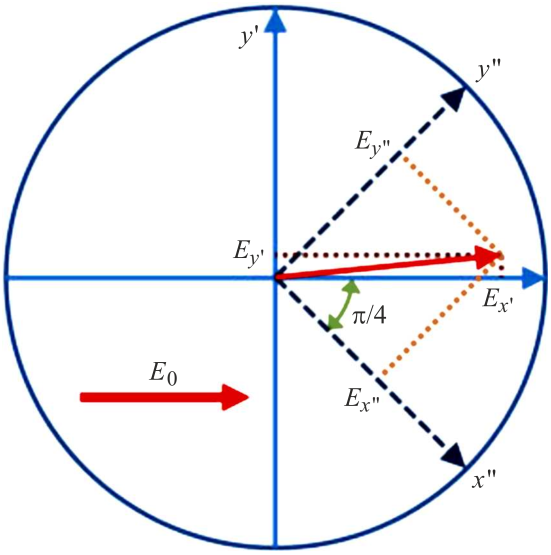

Figure 2. Balanced (differential) signal detection.

state with $N = 2(2I + 1)$ Zeeman levels, this system looks as follows:

$$\begin{cases} \frac{dn_1}{dt} = Q - R_1 \cdot n_1, \\ \frac{dn_2}{dt} = Q - R_2 \cdot n_2, \\ \dots \\ \frac{dn_N}{dt} = Q - R_N \cdot n_N, \\ \sum\limits_{m=1}^{N} = n_m = 1, \end{cases} \quad (5)$$

where $m = 1 \dots N$ is the index, n_m is the m level population, R_m is the total depopulation rate of level m, Q is the total level population rate due to relaxation of both excited and ground states:

$$R_m = P_{m,m} \cdot r_x + P_{m,m-1} \cdot r_{C-} + P_{m,m+1} \cdot r_{C+} + \gamma$$

$$= P_{m,m} \cdot r_x + \frac{1}{2}(P_{m,m-1} + P_{m,m+1}) \cdot r_y + \gamma,$$

$$Q = \frac{1}{N}\left(\sum_{m=1}^{N} R_m \cdot n_m\right) \quad (6)$$

γ is the ground state level relaxation rate, $r_x, r_y = r_{C+} + r_{C-}$, $r_{C+} = r_{C-}$ are the excitation rates proportional to the corresponding intensities of linear and circular pumping light components; $P_{i,j}$ are the relative probabilities of absorption of light with single intensity and corresponding polarization (circular polarization for transitions with the quantum number variation $\Delta m_F = j - i = \pm 1$, linear polarization along x — for transitions $\Delta m_F = j - i = 0$) by the ground state sublevels forming matrix $\mathbf{P}$. The theory for calculating $P_{i,j}$ is described in [14]. Tabulated values of the relative absorption probabilities for transitions in the structure of D_1- and D_2-lines of alkali metals are given in [15]. In the following calculations, we will use dimensionless pumping light intensities normalized to γ [16]: $I_{0x} = r_x/\gamma$, $I_{0y} = r_y/\gamma$, $I_0 = I_{0x} + I_{0y}$. Physical significance of I_0 is the relative light broadening of the ground state level.

Solution of (5) shall be found for a stationary case, for which derivatives with respect to time in (5) are set to zero. For further absorption calculation, two methods may be used: either directly by summing the absorption (using the probability coefficients given above) from all involved levels or by expansion of the medium polarization in spherical moments followed by multiplying the medium polarization matrix by the light polarization matrix [9,10]. These two methods shall yield the same results, but the second method is convenient in that it allows alignment (second-order moment) to be separated from orientation (first-order moment) and higher-order moments.

The resulting absorption vector components can generally be written as follows:

$$K_x(I_{0x}, I_{0y}) = K_0\left(1 - \frac{A_x(I_{0x}, I_{0y})}{1 + B_x(I_{0x}, I_{0y})}\right),$$

$$K_x(I_{0x}, I_{0y}) = K_0\left(1 - \frac{A_y(I_{0x}, I_{0y})}{1 + B_y(I_{0x}, I_{0y})}\right), \quad (7)$$

where A_x, B_x, A_y, B_y are polynomials in I_{0x} and I_{0y} with constant summands in them equal to zero. Exact solution for the system with three ground state sublevels contains only first-order polynomials. Solutions for multilayer systems contain higher-degree polynomials (5th degree for the isolated transition $F = 4 \leftrightarrow F' = 3$ in Cs), but in the weak pumping intensity approximation, the first orders of expansion in intensity are sufficient.

Then, by substituting (7) in (2) and using (1)–(4), we obtain expressions for the intensity and polarization of the test light transmitted through the cell.

In what follows, we will consider a single-beam scheme in which the pump light simultaneously serves as a probe beam. The total signal S_T measured in the transmitted light is merely equal to the cell output intensity:

$$S_T(I_0, \varphi_0) \equiv I(I_0, \varphi_0). \quad (8)$$

To measure the dichroism ΔK, two measurements are required — at $\varphi_0 = 0$ and $\varphi_0 = \pi/2$, respectively, modulation of either polarization direction or MF vector direction is required. The (x, y) coordinate system coordinates is still referenced to the MF direction.

Signal S_B in the balanced scheme may be defined in the same way. Let's conduct differential measurement by dividing the beam into two components with perpendicular polarizations and initially equal intensities. Axis of a polarization-splitting element (for example, polarization cube, PBS) is set at the angle $\pi/4$ to the initial beam polarization azimuth, component intensity is measured by two photodetectors whose signals are subtracted for measuring signal S_B and summed for measuring signal S_T.

Let's introduce two new coordinate systems: a system (x', y') related to the incoming beam azimuth ($\mathbf{E} \parallel \mathbf{x}'$) and a system (x'', y'') related to the photodetector (Figure 2). In the (x'', y'') coordinate system, the recorded signals S_T and S_B are expressed as follows:

$$S_T = I''_y + I''_x = E''^2_y + E''^2_x,$$
$$S_B = I''_y - I''_x = E''^2_y - E''^2_x \quad (9)$$

Transition to the (x', y')coordinate system related to the beam polarization plane and to the (x, y) coordinate system related to the field is performed through a standard transformation (rotation at $\pi/4$), wherein

$$S_T = I'_x + I'_y$$
$$S_B = -2\sqrt{I'_x \cdot I'_y} \quad (10)$$

and inverse transformation

$$I_{X'} = \frac{1}{2}\left(S_T + \sqrt{S_T^2 - S_B^2}\right)$$
$$I_{Y'} = \frac{1}{2}\left(S_T - \sqrt{S_T^2 - S_B^2}\right) \quad (11)$$

Signal S_T, as could be expected, doesn't depend on the coordinate system. The signal S_B is defined by the beam polarization plane rotation angle $\Delta\varphi = \varphi - \varphi_0$

$$S_B = -\frac{1}{2}\sin(2\Delta\varphi). \quad (12)$$

In the case of $\Delta\varphi \ll 1$, which is almost always met for LD signals, $S_B \sim \Delta\varphi$. Thus, both signals S_T and S_B may be represented independently on the coordinate system:

$$S_T = I,$$
$$S_B = -I \cdot \Delta\varphi. \quad (13)$$

Simultaneous measurement of signals S_B and S_T provides information about light intensity and rotation angle. From (1)–(3) it follows that $\Delta\varphi$ in the first linear approximation is proportional to ΔK, therefore, the measurement of signal S_B in particular conditions ($\varphi_0 \neq \pi/2$, where $n = 0, 1, 2\ldots$) is able to provide LD data just in one measurement. This obvious advantage of the balanced LD signal detection method, namely, the absence of the need for modulation of the relative MF and polarization directions, makes it possible to implement LD signal recording at the zero frequency.

However, in practice some factors, among which the excess laser noise whose spectral density grows as the frequency decreases is the primary factor, cause to use methods of signal transfer from the zero frequency to higher frequencies. For this, we have used the MF vector direction modulation that is technically easier than the light polarization azimuth modulation, while doesn't require a sophisticated recording scheme. A situation is be described

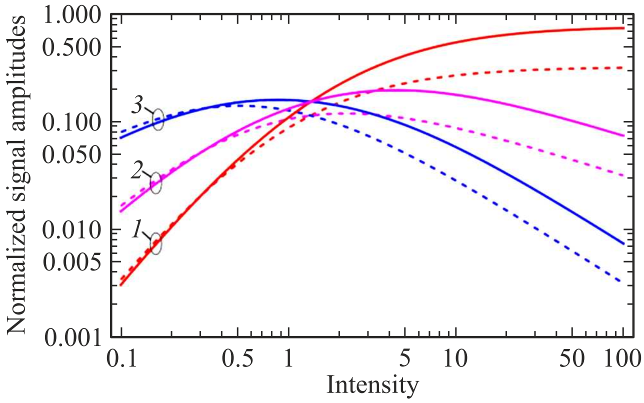

Figure 3. In the Cs atom model depending on the dimensionless pumping intensity I_0 in the single-beam scheme with unit optical density ($K_0 = 1 - 1/e$): red lines (*1*) — absolute value of signals A_{ST} and A_{SB}, purple lines (*2*) — signals $A_{ST}/\sqrt{I_{ph}}$ and $A_{SB}/\sqrt{I_{ph}}$ assigned to the root of I_{ph} on the photodetector (proportional to the maximum achievable signal-to-noise ratio), blue lines (*3*) — signal A_{ST}/I_{ph} and A_{SB}/I_{ph} assigned to I_{ph} on the photodetector.

below when the MF vector slowly (compared with the Cs ground state relaxation rate) rotates in plane perpendicular to the beam propagation direction; amplitudes A_{ST} and A_{SB} of variation of the recorded signals S_B and S_T give the information about ΔK. For practical purpose, it is then sufficient to limit the MF vector direction modulation by two angles providing the maximum signal spread.

Considerable advantage of the balanced method is in that it effectively suppresses the contribution of laser intensity fluctuations. This method is widely used for detecting optical orientation; however under conditions of optical orientation, the signal in the balanced scheme is induced by the circular birefringence effect and the rotation angle is not limited in any way — polarization plane in an optically-dense cell with effective pumping may perform dozens of complete revolutions. Anisotropic absorption caused by the LD effect according to (3) is also capable of inducing polarization rotation if this polarization is initially oriented at an angle to the magnetic field vector [13]. However, this rotation is limited to „pressing" of the polarization plane to one of the axes; therefore, it shall never exceed $\pi/4$ in any circumstances. And if the dichroism effect smallness compared with the total absorption is considered, then significant rotation ranges in the thick layer are followed by significant absorption of both components and, consequently, by decrease in the absolute signal value. Nevertheless, as will be shown below, the balanced scheme in some conditions prevails not only in noise suppression, but also in the absolute signal value.

Figure 3 shows peak-to-peak values A_{ST} and A_{SB} (calculated as the difference of maximum and minimum values with variation of the angle φ in the range from 0 to 2π) of S_T and S_B, relative values A_{ST}/I_{ph} and A_{SB}/I_{ph} as well as$A_{ST}/\sqrt{I_{ph}}$ and $A_{SB}/\sqrt{I_{ph}}$ proportional to the signal-to-noise ratio on the assumption of the shot nature of noise.

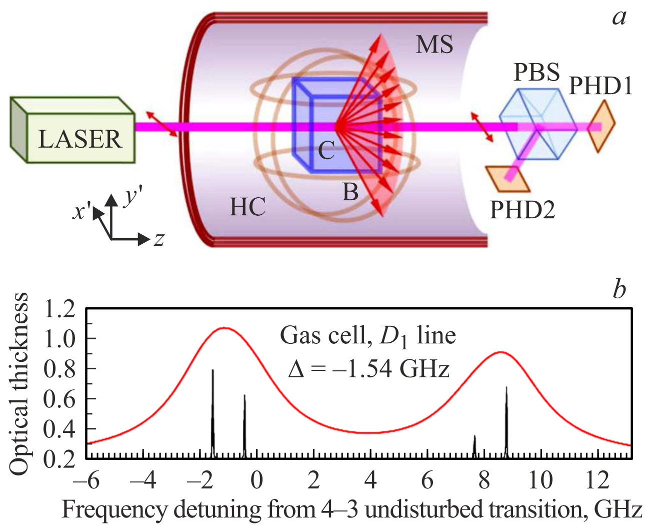

Figure 4. *a* Experimental setup. Magnetic field in coils rotates in the $0x'y'$ plane. (*b*) Calculated absorption spectrum of Cs (D_1-line) in the cell filled with 200 Torr N_2; frequency is counted from the unperturbed transition $F = 4 \leftrightarrow F' = 3$.

These values were calculated using the Cs atom model for the cell with buffer gas (nitrogen) pressure of 200 Torr. The pumping intensity I_0 is hereinafter normalized to the ground state level relaxation rate γ.

It can be seen that when $I_0 \gg 1$ the balanced detection method provides 2 to 3 times better signal-to-noise ratios; with the maximum signal-to-noise ratio provided at $I_0 \approx 5$. Provisions of this sections will be tested experimentally below.

Experiment

Total (S_T) and differential (S_B) absorption signals in the cells with Cs vapor in the Voigt geometry were measured experimentally depending on the angle between the magnetic field vectors and pumping light polarization azimuth (the same light served as the probe light). Magnetic field strength was selected such that the Larmor frequency ω_L was much higher than the relaxation rate γ of the Cs ground state in the cell. The polarization azimuth was fixed and the magnetic field vector rotated in the plane perpendicular to the beam (Figure 4), while the rate of rotation ω_R was much lower than the ground state relaxation rate: $\omega_R \ll \gamma \ll \omega_L$.

VitaWave's laser set to the D_1-line of Cs (wavelength 895 nm) was used as the pumping/detection source. Measurements were performed in a gas cell filled with 200 Torr N_2. Internal dimensions of the cubic cell were $5 \times 5 \times 5\,\mathrm{mm}^3$, effective beam cross-section was $3\,\mathrm{mm}^2$. Signals S_T and S_B were studied at various cell temperatures, detuning and light intensities. For detailed description of the main setup components (shield, optical pumping scheme, etc.), see [11,17,18].

For interpretation of the obtained results, the measured pumping power values were to be converted into the dimensionless intensity I_0. For this, according to [19,20], we calculated the atomic vapor concentration n_{Cs}, dark relaxation rate γ and, according to [16,21], light broadening for the cell used. It is shown that in the temperature range 76–107°C the design dark relaxation rate logarithm γ can be accurately taken as proportional to temperature.

Note that according to [21] (page 27, 28) the bleaching phenomenon leads to inapplicability of the Bouguer–Lambert law to the atomic system of interest: light absorption in it is linearly proportional to the optical thickness with reasonable accuracy.

Comparison of theoretical predictions with experimental predictions is shown in Figure 5. Laser frequency was shifted by 2.6 GHz downwards from the transition frequency of the $F = 4 \leftrightarrow F' = 3$ D_1-line of Cs in the vacuum cell at 95°C. Consequently, this frequency was shifted by ~ 1.2 GHz downwards with respect to the transition frequency $F = 4 \leftrightarrow F' = 3$ in the studied cell with nitrogen pressure equal to 200 Torr.

Figure 5 demonstrates good qualitative and quantitative agreement between the theory and experiment. In particular, it follows from the figure that the theory not only adequately predicts the type of angular dependences, but also quite accurately shows the ratios of their amplitudes (absolute value of theoretical signals was fitted by selecting a common value of I_0 for them). Figure 5 shows that the extrema of S_T and S_B are reached at angles other than $\pm 90°$. Thus, the optimum angles in the given medium for S_T are equal to 0° and 55–60°, and for S_T are 0° and 55–60°, and for S_B are $\pm 25°$.

Note that the experimental dependences in Figure 5 appear to be smoothed a little compared with the theoretical ones. The most probable cause behind this is that the theory does not take into account the optical layer thickness, while the cell in these conditions is certainly optically thick, and transmission of 60–70% in the absorption line peaks in the cell is implemented only due to the nonlinear bleaching effects.

Then, the theoretically calculated dependences of the normalized signals A_{ST}/I_0 and A_{SB}/I_0 on pumping intensity in the single-beam scheme were compared with the experimental data (Figure 6). Signal amplitudes measured at five temperatures were recalculated to the same optical density.

Figure 6 identifies good coincidence between the theory and experiment; in particular, the main conclusion of the previous section concerning the comparative amplitude of S_T and S_B is confirmed: at high ($I_0 > 1$) pumping intensities, detection of the balanced signal S_B turns to be preferable by the amplitude criterion and, consequently, by the signal-to-noise ratio, especially as it allows suppression of the pumping light source intensity noise.

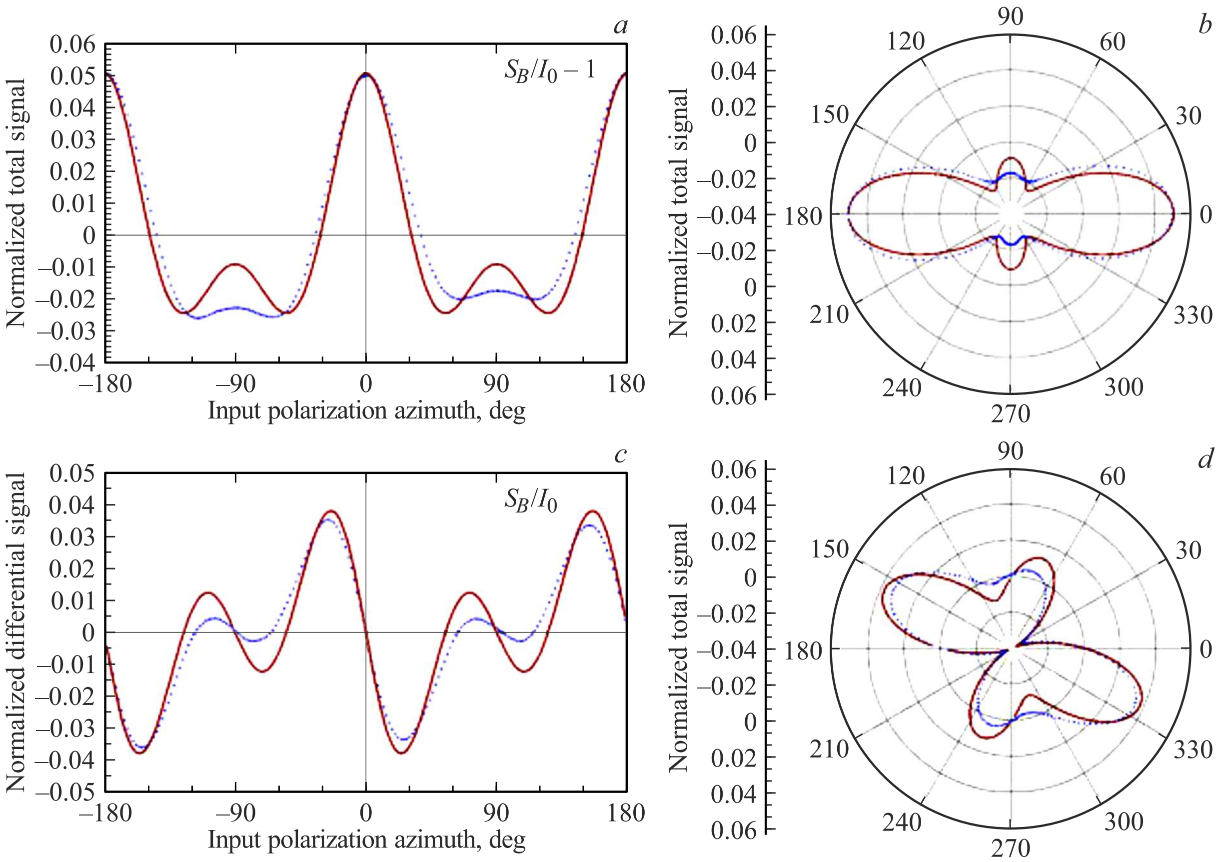

Figure 5. Theoretical (solid lines) and experimental (dots) dependences of normalized signals S_T/I_0-1 (a, b) and S_B/I_0 (c, d).

Conclusions

This work provides basic information about linear dichroism signals induced in alkali metal vapor during pumping by linearly polarized resonance light propagating perpendicularly to the magnetic field; gives the basis for theoretical calculation of the linear dichroism signals in cells with buffer gas that ensures complete mixing of excited states, and addresses the fundamental techniques of detecting these signals. Theoretical model of stationary alignment in the buffer gas cell has been built, angular dependences of LD signals in the single-beam scheme have been investigated using both the traditional and balanced detection method. Good qualitative and quantitative agreement between the theory and experiment has been demonstrated. It has been shown theoretically and supported experimentally that detection of the balanced signal S_B for applications using relatively high $(I_0 > 1)$ pumping light intensities was preferable not only because it allowed suppression of the pumping light source intensity noise, but also by the achievable signal-to-noise ratio criterion. The obtained results can be used in practical applications, such as quantum sensors based on the alignment effect and systems for precision stabilization of the frequency of laser radiation.

Acknowledgments

The authors are grateful to V.S. Zapasskii for promotion of the transverse linear dichroism effects and useful discussions.

Conflict of interest

The authors declare that they have no conflict of interest.

References

[1] C.L. Degen, F. Reinhard, P. Cappellaro. Rev. Mod. Phys., **89** (3), 035002 (2017). DOI: 10.1103/RevModPhys.89.035002

[2] G.M. Tino. Quantum Sci. Technol., **6** (2), 024014 (2021). DOI: 10.1088/2058-9565/abd83e

[3] G.M. Tino, M.A. Kasevich. *Atom Interferometry* (IOS Press, 2014) V. 188.

[4] T.K. Paraíso, R.I. Woodward, D.G. Marangon, V. Lovic, Z. Yuan, A.J. Shields. Advanced Quantum Technologies, **4** (10), 2100062 (2021). DOI: 10.1002/qute.202100062

[5] F. Schreck, K. van Druten. Nat. Phys., **17** (12), 1296 (2021). DOI: 10.1038/s41567-021-01379-w

[6] A. Nagel, L. Graf, A. Naumov, E. Mariotti, V. Biancalana, D. Meschede, R. Wynands. Europhys. Lett., **44** (1), 31 (1998). DOI: 10.1209/epl/i1998-00430-0

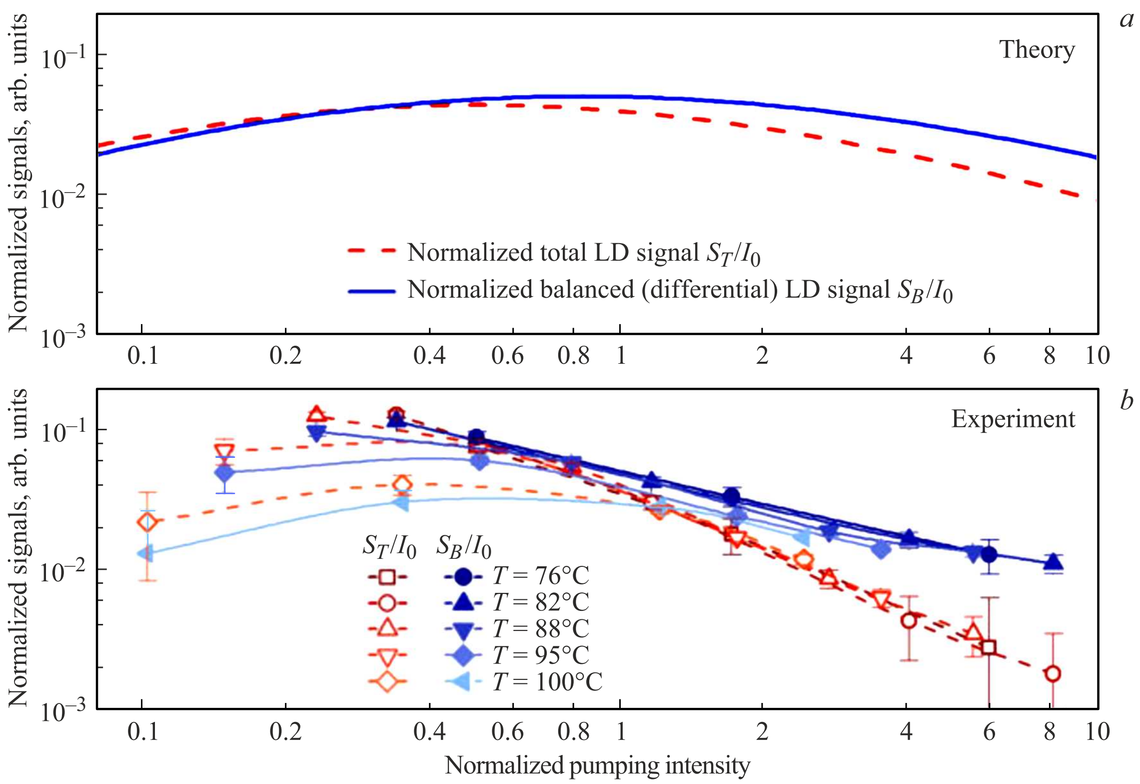

Figure 6. (a) Theoretical dependences of the normalized total (dashed) and balanced (solid lines) signals A_{ST}/I_0 and A_{SB}/I_0 in the model depending on the pumping intensity in the single-beam scheme; (b) the same signals in the experiment at different cell temperatures; signal amplitudes were recalculated to the same optical density.

[7] J. Vanier. Appl. Phys. B, **81** (4), 421 (2005). DOI: 10.1007/s00340-005-1905-3

[8] M. Fleischhauer, A. Imamoglu, J.P. Marangos. Rev. Mod. Phys., **77** (2), 633 (2005). DOI: 10.1103/RevModPhys.77.633

[9] A. Omont. Progress in Quantum Electronics, **5**, 69 (1977). DOI: 10.1016/0079-6727(79)90003-X

[10] *Density Matrix Theory and Applications*, ed. by K. Blum (Springer, Berlin, Heidelberg 2012), 115–163. DOI: 10.1007/978-3-642-20561-3_4

[11] M.V. Petrenko, A.S. Pazgalev, A.K. Vershovskii, Photonics 2024, **11** (10), 926 (2024). DOI: 10.3390/photonics11100926

[12] D. Budker, W. Gawlik, D.F. Kimball, S.M. Rochester, V.V. Yashchuk, A. Weis. Rev. Mod. Phys., **74** (4), 1153 (2002). DOI: 10.1103/RevModPhys.74.1153

[13] A. Meraki, L. Elson, N. Ho, A. Akbar, M. Koźbiał, J. Kołodyń ski, K. Jensen. Phys. Rev. A, **108** (6), 062610 (2023). DOI: 10.1103/PhysRevA.108.062610

[14] E.B. Alexandrov, M.P. Chaika, G.I. Khvostenko. Interference of atomic states (Springer, 1993) V. 7.

[15] Steck D.A. http://steck.us/alkalidata [Electronic source], 2003. URL: http://steck.us/alkalidata

[16] A.K. Vershovskii, A.S. Pazgalev. Tech. Phys., **53** (5), 646 (2008). DOI: 10.1134/S1063784208050198

[17] M.V. Petrenko, A.S. Pazgalev, A.K. Vershovskii. Phys. Rev. Appl., **15** (6), 064072 (2021). DOI: 10.1103/PhysRevApplied.15.064072

[18] M.V. Petrenko, A.S. Pazgalev, A.K. Vershovskii. IEEE Magnetics Lett., **12**, 8104605, 1 (2021). DOI: 10.1109/LMAG.2021.3132851

[19] R. Gary. *Vapor pressure of the chemical elements* (Elsevier, 1963). DOI: 10.1002/ange.19640761537

[20] W. Happer, T.G. Walker, Y.-Y. Jau. *Optically Pumped Atoms* (Wiley, 2010). DOI: 10.1002/9783527629503

[21] S.J. Seltzer. *Developments in alkali-metal atomic magnetometry* (Princeton University, 2008).

Translated by E.Ilinskaya